

On the Nature of Conformational Transition in Poly(ethylene glycol) Chains Grafted onto Phospholipid Monolayers

Valeria Tsukanova[†] and Christian Salesse*

Unité de Recherche en Ophtalmologie, Centre de Recherche du Centre Hospitalier de l'Université Laval, CHUQ, Ste-Foy, Québec, Canada G1V 4G2, and CERSIM, Université Laval, Ste-Foy, Québec, Canada G1K 7P4

Received: October 6, 2003; In Final Form: May 13, 2004

This study was aimed at understanding the nature of conformational transition(s) that occur in poly(ethylene glycol) chains with molecular weight 5000 (PEG5000) grafted onto phospholipid monolayers. The study was performed with monolayers of PEG–phospholipid, DSPE–PEG5000, at the air/water interface and on solid substrates. Surface pressure and surface potential measurements together with ellipsometry and Brewster angle and atomic force microscopy were used to assess changes in the conformation and hydration of PEG5000 chains with increasing PEG grafting density. A comparative analysis of our experimental data suggests that neither the concept of the first-order pancake-to-brush conformational transition nor the model considering two subsequent transitions, namely, pancake-to-mushroom and mushroom-to-brush transitions, are adequate in describing conformational changes in the DSPE–PEG5000 monolayer at the air/water interface. At low grafting densities, PEG5000 chains did behave as grafted polymeric chains in a good solvent forming true 2D pancakes at the air/water interface. However, the conformation developed at high grafting densities was found to differ significantly from the PEG5000 brush in a good solvent. Its extension into the subphase was in far better agreement with the theoretical predictions for the height of PEG5000 brush in a theta solvent. This finding together with the decreasing absolute value of ψ_0 potential of DSPE–PEG5000 monolayer implies that conformational transition(s) in PEG5000 are accompanied by changes in interactions of PEG monomers with water molecules and by a substantial dehydration of PEG5000 chains. Conformational changes in grafted PEG5000 chains at the air/water interface are therefore interpreted as a transition from pancake to poorly hydrated brush conformation.

Introduction

Grafted chains of poly(ethylene oxide) (PEO), a synthetic water-soluble polymer, are used extensively for a variety of practical applications. In recent years, a lot of attention has been drawn to short-chain PEOs with molecular masses in the range of 1000–5000 Da, also known as poly(ethylene glycol)s (PEG).^{1–18} Poly(ethylene glycol) has significant potential for a number of biomedical applications as a compatibility enhancer in biological systems.^{1–3} This is primarily because PEG grafts have been shown to reduce the adsorption of proteins substantially,^{2–5} which is generally recognized as a first response of the immune system against foreign materials. The resistance to protein adsorption has therefore made PEGs particularly attractive for use as surface coatings to improve the biocompatibility of implanted medical devices and to prolong the in vivo circulation time of liposomes for drug delivery.^{1–3} However, interactions of PEG with proteins as well as what effect the properties of grafted PEG chains such as polymer molecular weight, grafting density, and conformation have on protein adsorption are not yet fully understood. A major problem that the studies on PEG-grafted surfaces are encountering is that the structure of PEG grafts is not easy to assess; therefore, it is often assumed rather than known. For instance, the conformation of PEG chains grafted onto membrane-mimetic

surfaces, which has been identified as a key factor in the resistance of PEG to the adsorption of proteins, is still a matter of debate.

For many biomedical applications, an attractive approach to grafting PEG chains is through the introduction of PEG–lipid conjugates into membrane-mimetic lipid structures (monolayers, bilayers, and liposomes).^{2–4,6–8} It is usually assumed that PEG chains grafted onto lipid membranes behave like polymeric chains grafted onto solid surfaces, stretching into brushes with increasing surface density.^{3,4,6,7,9,10} On the basis of this assumption, it is then suggested that the PEG brushes provide a steric repulsive barrier that prevents the adsorption of proteins onto the membrane surface.^{3,4,6,10} It is also presumed that for PEG brushes to be effective in reducing the adsorption of proteins they must be highly stretched and hydrated.^{4,10} Yet, given the nature of interactions that drive the self-assembly of membrane-mimetic lipid structures, it is rather questionable whether cohesive forces between aliphatic chains of the lipid part of PEG–lipid molecules are strong enough to compensate for the repulsion between stretching PEG chains that tends to squeeze some of the PEG–lipid molecules out of the membrane to relax the stretching. Indeed, despite a number of experimental efforts, there have been no results presented that unambiguously report the formation of brushes for PEG chains grafted onto lipid monolayers, bilayers, and liposomes.

In this study, we have focused on the conformation of poly(ethylene glycol) chains with molecular mass 5000 (PEG5000)

* Corresponding author. E-mail: Christian.Salesse@crchul.ulaval.ca.

[†] Present address: Department of Chemistry, York University, Toronto, Ontario, Canada.

grafted onto phospholipid monolayers at the air/water interface. Monolayers are the simplest membrane-mimetic surfaces. Being well-defined systems with many variable parameters, they provide exceptionally useful experimental models. For instance, with monolayers, an increase in grafting density can be performed in a well-controlled manner by compressing a PEG-grafted phospholipid monolayer at the air/water interface. In recent years, monolayers of phospholipids that are N-derivatized in the headgroup with PEG5000 have been widely used as models to study the properties of PEG5000 chains grafted onto membrane-mimetic surfaces.^{2,3,5,7,9–15} A lot of controversy, however, still exists over the conformation of grafted PEG5000 chains and how it changes with increasing surface density. In particular, as inferred from surface pressure–molecular area (π – A) isotherms, PEG5000-grafted phospholipid monolayers at the air/water interface undergo two transitions as the grafting density of PEG chains increases upon compression. The first transition shows up as a pseudoplateau at moderate surface pressures, whereas the second one appears at higher surface pressures as a slope discontinuity in the low-compressibility region of π – A isotherms.^{5,9,12,13,15} Although different interpretations were suggested in the literature, most of them associate the transitions in PEG5000-grafted phospholipid monolayers with conformational changes in PEG5000 chains. It is generally accepted that PEG5000 chains grafted onto phospholipid monolayers follow scaling behavior with a transition to the brush conformation at high grafting densities.^{3,5,7,9,11–13} The latter conclusion is usually made on the basis of the correlation between predictions of scaling theories for the thickness of the PEG5000 layer in the brush regime and measured thickness values for PEG5000-grafted phospholipid monolayers in the low-compressibility region of their isotherms (high grafting density regime).^{7,11} However, our previous study has shown that the second transition in a PEG5000-grafted phospholipid monolayer in fact corresponds to the monolayer collapse.¹⁵ The low-compressibility region therefore has nothing to do with the stretching of PEG5000 chains into brushes. Furthermore, the conformation of PEG5000 chains developed prior to collapse, although relatively elongated, was far less extended than that of brushes.¹⁵ Thus, these findings have brought up an old question: What is the nature of the conformational transition in PEG5000 chains grafted onto phospholipid monolayers at the air/water interface? Answering this question is obviously important to understanding the behavior of PEG chains grafted onto phospholipid surfaces as well as the causes and the driving forces of conformational transition(s) and the properties of the conformation that is eventually developed at high grafting densities.

To understand conformational transition(s) in PEG5000 chains grafted onto phospholipid monolayers better, we investigated the behavior of PEG5000–phosphatidylethanolamine at the air/water interface and in films transferred on solid substrates. Surface pressure and surface potential measurements together with ellipsometry and Brewster angle and atomic force microscopy were used to assess changes in the conformation and hydration of PEG5000 chains with increasing grafting density. On the basis of the comparison of our experimental data with theoretical predictions, conformations of the PEG5000 chain were identified at various grafting densities, and limits of different conformational regimes were determined. The results were analyzed in light of existing theoretical models. A new interpretation is suggested for conformational changes in PEG5000 chains grafted onto phospholipid monolayers.

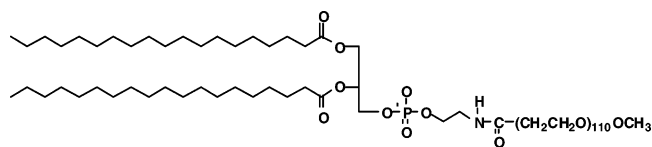


Figure 1. Chemical formula for the DSPE–PEG5000 molecule.

2. Materials and Methods

2.1. Materials. The poly(ethylene glycol)-grafted phospholipid with PEG average molecular mass of 5000, 1,2-distearoyl-*sn*-glycero-3-phosphatidylethanolamine-*N*-[poly(ethylene glycol) 5000] (DSPE–PEG5000), was purchased from Avanti Polar Lipids and used without further purification. Its chemical formula is presented in Figure 1. DSPE–PEG5000 monolayers were spread from chloroform solutions onto a bare water surface. The spreading solutions of DSPE–PEG5000 were prepared at a concentration of 0.1–0.4 mg/mL and stored in the dark at 4 °C. Chloroform was of HPLC grade (Omega, QC). In all experiments, unless mentioned otherwise, deionized water produced by a Nanopure water purification system was used as the subphase. The specific resistivity of water was $18 \times 10^6 \Omega \cdot \text{cm}$ (pH 5.6 in equilibrium with atmospheric carbon dioxide). The inorganic reagent, HCl, used in the experiments was Analar grade (Omega, QC).

2.2. Methods. A homemade Teflon-coated Langmuir trough with a movable barrier described elsewhere¹⁹ was used to study the PEG–phospholipid monolayers. The trough was thermostated and enclosed in a box. A filter paper Wilhelmy plate was used to measure surface pressure (π). The monolayer surface potential (ΔV) was detected with an ²⁴¹Am-coated ionizing electrode located 2 mm above the water surface, whereas the reference electrode made of platinum was immersed at the bottom of the trough. During monolayer compression, we recorded π and ΔV simultaneously. The surface pressure was detected to an accuracy of ± 0.1 mN/m, and the surface potential was measured to an accuracy of ± 15 mV.

Measurements of the thickness of DSPE–PEG5000 monolayers in situ at the air/water interface were performed using a homemade vibration-free Teflon-coated Langmuir trough interfaced with a conventional PCSA null ellipsometer. The trough was thermostated and enclosed in a box to minimize the possible contamination of the air/monolayer/water interface. The ellipsometer, described in detail elsewhere,²⁰ was capable of tracking azimuthal angles with a precision of 0.00034°. A 5-mW He–Ne laser operating at a wavelength of 632.8 nm was used as the light source. To record azimuthal angles, we stopped compression at a given surface pressure for 15–20 min.

A commercial Brewster angle microscope (Nanofilm Technologie GmbH, Göttingen, Germany) was used for the direct visualization of DSPE–PEG5000 monolayers at the air/water interface. The microscope was mounted on a NIMA film balance (Coventry, England). The frequency-doubled output of a Nd³⁺:YAG laser (532 nm, 20 mW) was used as the light source. The polarizer and analyzer were set to p polarization. The air/monolayer/water interface was illuminated at an angle of 53.1°. Light was focused on the monolayer with a 10 \times objective (Nikon, MPlan 10). Monolayer compression and BAM measurements were made simultaneously.

Tapping-mode atomic force microscopy (AFM) measurements were performed with a commercial Nanoscope IIIa (Digital Instruments, Santa Barbara, CA). Experiments were made in air at room temperature (20–25 °C) within 4 h after sample preparation as described in detail elsewhere.¹⁵ A 5 \times 5 (x, y) \times 2.5 (z)- μm^3 scan range was typically used for imaging.

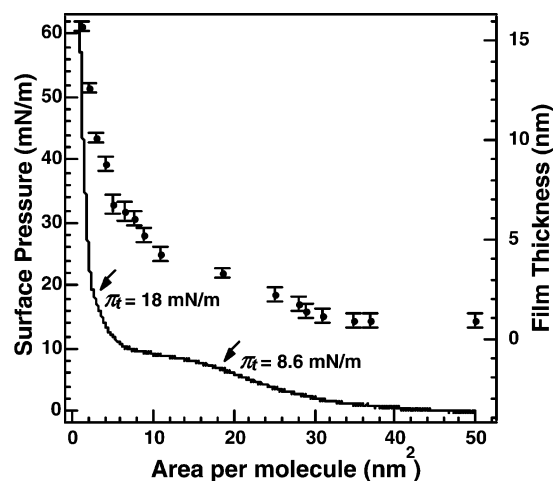


Figure 2. π -A isotherm of the DSPE-PEG5000 monolayer at the air/water interface. The isotherm was measured at 20 ± 1 °C and a compression speed of $1.25 \text{ nm}^2/\text{molecule} \cdot \text{min}$. Arrows indicate the onset of the first transition (isotherm plateau) at $\pi \approx 8.6 \text{ mN/m}$ and the second transition (high-pressure transition) at $\pi \approx 18 \text{ mN/m}$. Filled circles (●) show values for the thickness of DSPE-PEG5000 monolayer plotted vs area per molecule. The thickness values were calculated from ellipsometric data using a 5th-degree polynomial approach.²⁰ Error bars show the standard deviation from the average value obtained for each data point in a series of measurements performed with several monolayers.

To transfer DSPE-PEG5000 monolayers from the water surface onto a solid substrate, we employed the Langmuir-Blodgett deposition technique. All monolayers were deposited onto freshly cleaved mica in the upstroke mode.

All experiments were done at 20 ± 1 °C, unless specified otherwise.

3. Results

3.1. Surface Pressure (π -A) Isotherm. We have previously reported on the monolayer behavior of DSPE-PEG5000 at the air/water interface.¹⁵ In brief, the DSPE-PEG5000 monolayer exhibits the expanded-type isotherm.²¹ As seen in Figure 2, the π -A isotherm lift-off is observed at fairly large molecular areas ($\sim 50 \text{ nm}^2/\text{molecule}$). Then the surface pressure increases monotonically in the expanded region and reaches a plateau value below $18 \text{ nm}^2/\text{molecule}$. The plateau extends to an area of $\sim 8 \text{ nm}^2/\text{molecule}$ at a surface pressure of $\sim 8.6 \text{ mN/m}$. Upon further compression, we attain a region of low compressibility with rapidly increasing π , yet another discontinuity occurs in the slope of the isotherm in the 3.2 – $2.4 \text{ nm}^2/\text{molecule}$ region. This second plateau-like region at $\pi \approx 18 \text{ mN/m}$ can be referred to as the high-pressure transition. Our previous study showed that above this high-pressure transition the DSPE-PEG5000 film was no longer a monolayer.¹⁵ In the present report, we will focus mainly on the molecular organization in the DSPE-PEG5000 monolayer prior to collapse (below 18 mN/m), in particular, on how the conformation of the PEG5000 chains was changing with increasing grafting density upon compression in the 50 – $5 \text{ nm}^2/\text{molecule}$ region preceding the monolayer collapse.

3.2. Ellipsometric Measurements. The thickness of the DSPE-PEG5000 monolayer at the air/water interface was assessed by ellipsometry. At a fixed angle of incidence and wavelength, ellipsometry measures two parameters simultaneously, that is, angles Ψ (change in amplitude ratio due to reflection) and Δ (relative phase shift). Deviations of the two ellipsometric angles from values of $\bar{\Psi}$ and $\bar{\Delta}$ for a bare water

surface ($\delta\Psi = \Psi - \bar{\Psi}$ and $\delta\Delta = \Delta - \bar{\Delta}$) are related to the refractive index n and thickness d of the film.^{20,22,23} It has been shown²⁰ that precise absolute Ψ and Δ allow n to be separated from d by a numerical inversion procedure. Thus, film thickness, d , was calculated using the polynomial approach explicated elsewhere,²⁰ which gives solutions for both n and d directly from ellipsometric equations and experimental values of Ψ and Δ .

The filled circles in Figure 2 show values for the thickness of the DSPE-PEG5000 monolayer obtained at different molecular areas. In the 50 – $35 \text{ nm}^2/\text{molecule}$ region, the monolayer's thickness remained unchanged. The value of approximately 0.9 nm agrees well with values reported previously for expanded monolayers of PEOs.^{22,24} Then, below $30 \text{ nm}^2/\text{molecule}$, the monolayer's thickness starts to increase gradually. At the end of the π -A isotherm plateau, the thickness of the DSPE-PEG5000 monolayer was found in the range of 6.1 – 6.8 nm . These values are in good correlation with X-ray reflectivity data for the DSPE-PEG5000 monolayer reported elsewhere.¹¹ Upon further compression, slightly reducing the molecular area induced significant changes in d . As we showed previously, the reason for the abrupt increase in film thickness up to 15.8 nm observed in the low compressibility region of the π -A isotherm is the appearance of collapsed structures within the monolayer.¹⁵ The thickness data obtained in the low compressibility region are therefore irrelevant to the matter of the present report and will not be discussed in detail.

3.3. Brewster Angle and Atomic Force Microscopy of DSPE-PEG5000 Monolayers. BAM images captured from a DSPE-PEG5000 monolayer at the air/water interface displayed continuous gray fields from low surface pressures up to the end of the π -A isotherm plateau (data not shown). AFM images of DSPE-PEG5000 monolayers transferred onto mica were consistent with BAM images captured from the monolayer at the air/water interface. Indeed, similar to the BAM of the monolayer on the water surface, AFM performed with DSPE-PEG5000 monolayers transferred at various surface pressures showed that a homogeneous phase exhibiting a small height difference existed in the 50 – $5 \text{ nm}^2/\text{molecule}$ region of the π -A isotherm.¹⁵ Uniform topographic images were typical of DSPE-PEG5000 monolayers from low surface pressures up to the end of the isotherm plateau.

3.4. Surface Potential (ΔV -A) Isotherm and Dipole Moment for the PEG Moiety. Figure 3 shows the ΔV -A isotherm of the DSPE-PEG5000 monolayer at the air/water interface (curve a). For the purpose of comparison, the π -A isotherm of DSPE-PEG5000 on water is also shown in the same graph (curve c). As can be seen in the Figure, the surface potential starts to grow from its initial value of $+70 \text{ mV}$ at an area of $\sim 50 \text{ nm}^2/\text{molecule}$. Unlike phospholipid monolayers,^{25–27} the increase in ΔV on the lift off is not particularly sharp. The surface potential increases gradually in the 50 – $25 \text{ nm}^2/\text{molecule}$ region, reaching a maximum value of $+340 \text{ mV}$ at the plateau that extends to $8 \text{ nm}^2/\text{molecule}$. On further compression, ΔV decreases slowly, and a sudden drop is detected at an area of $\sim 2.2 \text{ nm}^2/\text{molecule}$ whereas below $1.4 \text{ nm}^2/\text{molecule}$ ΔV increases again.

Although the factors contributing to the monolayer's surface potential are complex and their theoretical estimation is still a matter of discussion, ΔV measurements have proven to be a source of valuable information about molecular organization at the air/water interface.^{14,16,18,26–32} For monolayers of amphiphilic compounds, a quantitative relationship between measured ΔV and normal components of group dipole moments

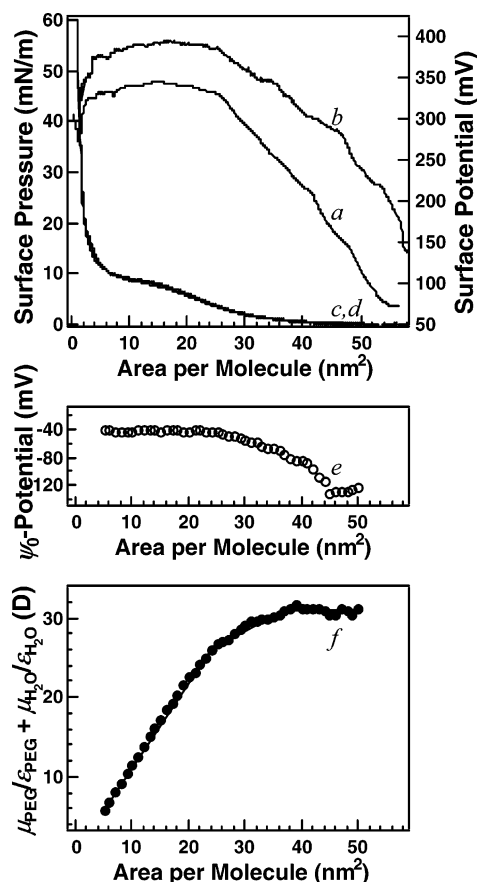


Figure 3. ΔV – A isotherms for the DSPE–PEG5000 monolayer measured on water (a) and on the acidic subphase at pH 1.9 (b). The experimental conditions are identical to those in Figure 2. π – A isotherms for the DSPE–PEG5000 monolayer on water and on the acidic subphase are also shown for comparison (curves c and d). Open circles (○) are the dependence of the ψ_0 potential on the area per molecule obtained for the DSPE–PEG5000 monolayer on water (e). Filled circles (●) are values of $\mu_{\text{PEG}}/\epsilon_{\text{PEG}} + \mu_{\text{H}_2\text{O}}/\epsilon_{\text{H}_2\text{O}}$ calculated from ΔV data using eq 2, and straight lines provide guides to the eye (f). To convert the calculated values of $\mu_{\text{PEG}}/\epsilon_{\text{PEG}} + \mu_{\text{H}_2\text{O}}/\epsilon_{\text{H}_2\text{O}}$ into debye units, the conversion factor $1 \text{ D} = 3.335 \times 10^{-30} \text{ C}\cdot\text{m}$ was applied.³²

is usually made using the Demchak–Fort three-layer capacitor model.^{29,30,32,33} The surface potential of a polymer monolayer can be considered to be a linear combination of group dipole moments, μ_i , of (1) terminal CH_3 groups, (2) hydrophilic headgroups, and (3) polymeric moieties and water molecules reoriented and polarized by the monolayer. In addition, when the monolayer is ionized, an electric double layer contributes to the surface potential, ΔV , with double-layer potential ψ_0 . Applying the Demchak–Fort approach, the surface potential for the DSPE–PEG5000 monolayer is thus written as

$$\Delta V = \frac{1}{\epsilon_0 A} \left(2 \frac{\mu_{\text{CH}_3}}{\epsilon_{\text{CH}_3}} + 2 \frac{\mu_{\text{C=O}}}{\epsilon_{\text{C=O}}} + \frac{\mu_{\text{PE}}}{\epsilon_{\text{PE}}} + \frac{\mu_{\text{PEG}}}{\epsilon_{\text{PEG}}} + \frac{\mu_{\text{H}_2\text{O}}}{\epsilon_{\text{H}_2\text{O}}} \right) + \psi_0 \quad (1)$$

where ϵ_0 is the permittivity of vacuum, A is the area per molecule, and μ_{CH_3} , $\mu_{\text{C=O}}$, μ_{PE} and μ_{PEG} are normal components of the dipole moments of the acyl chain terminal CH_3 group, the carbonyl C=O group of the glyceride part of the molecule, the phosphatidylethanolamine (PE) headgroup, and the PEG moiety, respectively. Because local polarizabilities depend on the medium immediately surrounding dipoles, we assigned a different effective dielectric constant, ϵ_i , to each of the layers.³³ The term $\mu_{\text{H}_2\text{O}}/\epsilon_{\text{H}_2\text{O}}$ is used to account for the reorientation and

polarization of water molecules induced by the PEG–phospholipid monolayer. It is generally admitted³⁰ that eq 1 deals with a number of parameters for which reliable values are difficult to obtain, if not impossible. However, to gain insight into the nature of conformational transitions of DSPE–PEG5000 at the air/water interface, only a few of them have to be analyzed on a comparative basis as discussed below.

Throughout the molecular area range of 50 – $5 \text{ nm}^2/\text{molecule}$, the ΔV – A isotherm of the DSPE–PEG5000 monolayer exhibits features that are typically observed in surface potential isotherms of PEG and PEO monolayers. A similar pattern where the surface potential increased gradually, achieving a maximum value at a plateau, followed by a decrease in ΔV was reported for a series of PEOs with molecular masses in the range of 200 – $100\,000$.^{14,16} Studying the effect of PEGs on the properties of phospholipid monolayers, Winterhalter et al.¹⁶ also noticed that, for large molecular areas, surface potentials were virtually identical to those produced by polymers in the absence of phospholipids. By contrast, as the molecular area was reduced to below $0.9 \text{ nm}^2/\text{molecule}$, the contribution of the phospholipid to ΔV became crucial. The latter is not surprising because a major contribution to the phospholipid monolayer's ΔV is provided by terminal dipoles of alkyl chains when they are well ordered and oriented more upright at the interface.^{26,30,31} Given the fact that the ordering of alkyl chains requires close packing, which occurs when the area available per molecule in the monolayer is comparable with the cross-sectional area of an alkyl chain (0.19 nm^2),³⁴ we may assume that for DSPE–PEG5000 the contribution of the phospholipid part of the molecule compared to the measured ΔV is negligible at areas above $5 \text{ nm}^2/\text{molecule}$. Indeed, as judged by the shape of both the π – A and ΔV – A isotherms, it is more likely that at areas above $5 \text{ nm}^2/\text{molecule}$ the dominant contribution to the DSPE–PEG5000 surface potential comes from the normal dipole component of the PEG moiety and oriented water dipoles. Consequently, solving eq 1 for $\mu_{\text{PEG}}/\epsilon_{\text{PEG}}$ and $\mu_{\text{H}_2\text{O}}/\epsilon_{\text{H}_2\text{O}}$ we write

$$\frac{\mu_{\text{PEG}}}{\epsilon_{\text{PEG}}} + \frac{\mu_{\text{H}_2\text{O}}}{\epsilon_{\text{H}_2\text{O}}} = \epsilon_0 A (\Delta V - \psi_0) \quad (2)$$

We would like to stress that this equation is used in the present study only to estimate dipole contributions in the 50 – $5 \text{ nm}^2/\text{molecule}$ region. At areas below $5 \text{ nm}^2/\text{molecule}$, the group dipole moments of the phospholipid part of the DSPE–PEG5000 molecule undoubtedly should be considered. However, neither eq 1 nor eq 2 can be applied below $5 \text{ nm}^2/\text{molecule}$ because the film is no longer a monolayer.¹⁵

To calculate $\mu_{\text{PEG}}/\epsilon_{\text{PEG}} + \mu_{\text{H}_2\text{O}}/\epsilon_{\text{H}_2\text{O}}$, the ψ_0 potential of the DSPE–PEG5000 monolayer should be determined. As suggested by Dynarowicz-Latka et al.,²⁸ a portion of ΔV that is associated with the double-layer potential can be found by a comparison of the surface potentials of a nonionized monolayer on an acidic subphase and an ionized monolayer on pure water. Given an intrinsic pK_a of 0.32 – 0.7 for the phosphatidyl group,³¹ it is reasonable to expect PE headgroups to be completely neutralized by protons at a subphase $\text{pH} \leq 2$. Hence, the ΔV – A isotherm of a DSPE–PEG5000 monolayer spread onto a subphase containing HCl at pH 1.9 was measured (curve b in Figure 3). As seen in Figure 3, the shape of both surface pressure and surface potential isotherms was not altered to any significant extent when the acidic subphase was used. Indeed, the π – A isotherm obtained on the acidic subphase (curve d in Figure 3) is virtually identical to that measured on water (curve c). In the case of the surface potential, however, ΔV for the nonionized

monolayer on the acidic subphase was always higher than that for DSPE-PEG5000 on water. The lower surface potential for the monolayer spread on water is attributed to the negative ψ_0 potential of the double layer formed by PE headgroups and protons because the monolayer is partially ionized at pH 5.6. Subtracting the ΔV - A isotherm on the acidic subphase from curve a in Figure 3, we obtained the dependence of the ψ_0 potential on the area per molecule for the DSPE-PEG5000 monolayer at the air/water interface (curve e, Figure 3). Because the values for the ψ_0 potential at different molecular areas are known, the value of $\mu_{\text{PEG}}/\epsilon_{\text{PEG}} + \mu_{\text{H}_2\text{O}}/\epsilon_{\text{H}_2\text{O}}$ can be readily determined using eq 2.

The dependence of $\mu_{\text{PEG}}/\epsilon_{\text{PEG}} + \mu_{\text{H}_2\text{O}}/\epsilon_{\text{H}_2\text{O}}$ as a function of area per molecule is depicted in Figure 3 (curve f). It should be mentioned that to extract reliable values for $\mu_{\text{PEG}}/\epsilon_{\text{PEG}}$ and $\mu_{\text{H}_2\text{O}}/\epsilon_{\text{H}_2\text{O}}$ from the overall dipole sum, $\mu_{\text{PEG}}/\epsilon_{\text{PEG}} + \mu_{\text{H}_2\text{O}}/\epsilon_{\text{H}_2\text{O}}$, a number of dipolar interactions associated with the hydration of the monolayer must be considered. However, as demonstrated by previous studies,^{35,36} water is intimately involved in the organization of PEG-phospholipids at the air/water interface and conformational transitions in polymeric chains. The uniform orientation of phospholipid headgroup dipoles alters the orientation of water dipoles because it generates fields that polarize bulk water adjacent to the monolayer and causes significant perturbations that persist as far as 3–3.5 nm below the phospholipid/water interface.³⁷ Furthermore, water is able to pack PEG chains, bridging oxygen atoms of $-(\text{CH}_2\text{CH}_2\text{O})-$ monomers and facilitating the formation of polymer coils.^{35,36} It is thus clear that a model analyzing all components that should be properly accounted for has yet to be developed. Meanwhile, on a comparative basis, variations in $\mu_{\text{PEG}}/\epsilon_{\text{PEG}} + \mu_{\text{H}_2\text{O}}/\epsilon_{\text{H}_2\text{O}}$ upon decreasing molecular area can indicate that changes in the hydration and/or conformation of PEG chains have occurred.

4. Discussion

Like poly(ethylene oxide) and most PEO- and PEG-lipid conjugates, DSPE-PEG5000 readily spreads at the air/water interface. As reflected by the expanded-type π - A isotherm shown in Figure 2, the monolayer behavior of DSPE-PEG5000 is profoundly influenced by the grafted polymeric chain. Typical of monolayers of PEOs and PEGs,^{5,6,9,11–18,21,22,24,38–41} the surface pressure is detectable for the DSPE-PEG5000 monolayer at fairly large molecular areas. A pseudoplateau appears in the isotherm at $\pi \approx 8.6$ mN/m, indicating a conformational transition in the polymeric moiety upon compression.^{9,15} Yet, by contrast to monolayers of PEOs that collapse at $\pi \approx 10$ mN/m,^{21,42} the isotherm of DSPE-PEG5000 exhibits a distinct low-compressibility region with the surface pressure increasing rapidly up to ~ 63 mN/m. This low-compressibility region was associated in previous studies with the stretching of grafted PEG5000 chains into brushes.^{7,9,11–13} However, our recent study¹⁵ has shown that, in fact, similar to monolayers of PEOs, the DSPE-PEG5000 monolayer does not sustain high surface pressures and collapses at $\pi \approx 18$ mN/m, at which the second discontinuity appears in the isotherm slope (high-pressure transition in Figure 2). Indeed, both BAM and AFM displayed budding collapsed structures that started to appear in the DSPE-PEG5000 monolayer slightly above the isotherm plateau.¹⁵ This finding, therefore, suggests that the low-compressibility region in the DSPE-PEG5000 isotherm has nothing to do with the stretching of PEG5000 chains into brushes. The question that remains is whether the stretching of PEG5000 chains grafted onto phospholipid monolayers into brushes occurs at all. Is it possible that PEG5000 brushes are developed prior to the

collapse of the DSPE-PEG5000 monolayer, for instance, at the end of the isotherm plateau? To answer these questions, one has to discuss in detail possible conformations of PEG5000 chains at the air/water interface and the nature of the transition that occurs in the isotherm plateau.

In general, for grafted PEO and PEG chains, three major conformational regimes have been identified. These three regimes can be referred to as (1) a truly 2D dilute pancake regime, (2) mushrooms, and (3) brushes.^{3–7,9,11–13,17,42} Accordingly, the behavior of grafted PEO and PEG chains at surfaces and interfaces is usually discussed in terms of transitions between these three conformations. In particular, the pseudo-plateau typically observed in isotherms of PEG-grafted lipid monolayers at the air/water interface was attributed to a pancake-to-mushroom conformational transition in the polymeric moiety.^{9,12,17} Alternative concepts interpreted the plateau in isotherms of PEO-grafted copolymer monolayers as a transition from pancake to brush conformation.^{38–41} However, which concept is the most adequate in describing conformational transition(s) in PEG5000 chains grafted onto phospholipid monolayers at the air/water interface is unclear.

4.1. Conformation of PEG5000 Chains in the Expanded Monolayer. For the DSPE-PEG5000 monolayer, the π - A isotherm lift off is observed at an area of ~ 50 nm²/molecule. Given the projected area of each hydrated $-(\text{CH}_2\text{CH}_2\text{O})-$ monomer of approximately $0.35 \text{ nm} \times 0.9 \text{ nm}$,^{8,22,24} this area of 50 nm^2 /molecule is large enough to accommodate all $-(\text{CH}_2\text{CH}_2\text{O})-$ monomers of each PEG5000 chain (containing 110 monomers) at the interface. It is therefore very likely that, upon spreading, polymeric chains indeed adopt a 2D pancake conformation. The same conclusion comes from the ellipsometric measurements of monolayer thickness. As seen in Figure 2, at the beginning of the isotherm, a value of ~ 0.9 nm was found for the thickness of the DSPE-PEG5000 monolayer. Similar thickness values were reported for expanded monolayers of PEOs of different molecular masses.^{22,24} This implies that for large molecular areas every $-(\text{CH}_2\text{CH}_2\text{O})-$ monomer of PEO and PEG chains is maintained at the interface. As a result, a true 2D monolayer is formed with the thickness determined primarily by the thickness of the hydrated $-(\text{CH}_2\text{CH}_2\text{O})-$ monomer. Hence, the molecular area range where such a truly 2D monolayer of DSPE-PEG5000 exists can be roughly estimated from ellipsometric data. As seen in Figure 2, the thickness of the DSPE-PEG5000 monolayer remained at 0.9 nm throughout the 50 – 35 nm^2 /molecule region. This indicates that the pancake conformation adopted by PEG5000 chains at the air/water interface was not altered to any significant extent upon compression to $\sim 35 \text{ nm}^2$ /molecule.

The analysis of the π - A isotherm in Figure 2 in terms of the virial expansion approach^{39,41} and self-avoiding walk model^{38,39,41} yielded virtually the same limits for the pancake regime in the DSPE-PEG5000 monolayer. In general, the surface pressure of an expanded polymer monolayer is given by

$$\pi \propto \left(\frac{1}{A}\right)^y \quad (3)$$

where y is the exponential factor depending on excluded volume and space dimensionality parameters.^{38,41} In the true pancake regime, the monolayer's surface pressure originates solely from lateral repulsion between polymeric chains extended at the interface and is a function of $(1/A)^2$.^{38,39,41} However, upon further compression of the expanded monolayer, interactions between polymeric chains at the air/water interface may become sig-

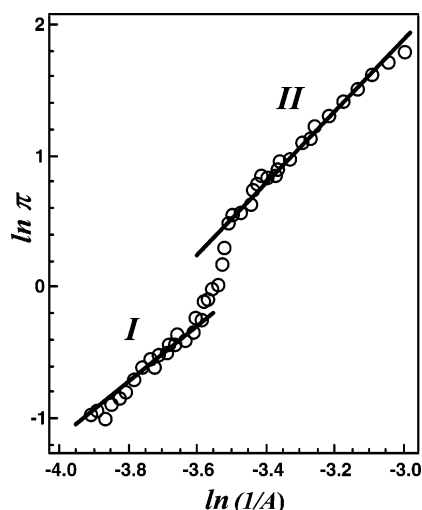


Figure 4. Analysis of the π - A isotherm.^{39,41} Surface pressure, π , vs the reciprocal of molecular area, $1/A$, on a double-logarithmic scale for the expanded DSPE-PEG5000 monolayer. Open circles (○) are experimentally measured surface pressures, whereas solid lines are linear fits defining two different conformational regimes. (See explanations in the text.) Regime I extends from 50 to ~ 37 nm²/molecule; a value of 1.97 obtained for the exponential factor γ from the slope of the linear fit suggests that this is the true pancake regime.^{39,41} Regime II is characterized by $\gamma \approx 2.5$ thus implying that polymeric chains of DSPE-PEG5000 molecules form a quasi-3D layer in the 34–25 nm²/molecule region of the π - A isotherm.^{38,39,41}

nificant. These interactions may alter the conformational order causing either (1) entanglement and interpenetration of polymer chains remaining at the interface or (2) expulsion of some $-(\text{CH}_2\text{CH}_2\text{O})-$ segments from the interface into the subphase resulting in the formation of a quasi-3D layer.^{39,41} According to Bijsterbosch et al.³⁸ and Fauré et al.,^{39,41} for the 2D entangled layer, $\pi \propto (1/A)^3$ behavior is expected, whereas in the case of the quasi-3D layer, a value of $\gamma = 2.25$ is predicted. Hence, to distinguish possible conformational regimes, we estimated the value of the exponential factor γ by plotting the experimentally measured monolayer surface pressure versus $1/A$ on a double-logarithmic scale. As seen in Figure 4, the $\ln \pi$ versus $\ln 1/A$ plot for the expanded DSPE-PEG5000 monolayer (between 50 and 18 nm²/molecule) exhibits two distinct regimes. For each of these regimes, we calculated values of the exponential factor γ from the slope of linear fits (solid lines in Figure 4). In regime I corresponding to the 50–37 nm²/molecule region of the π - A isotherm, we obtained a value of $\gamma = 1.97$. This finding implies $\pi \propto (1/A)^2$ behavior at large molecular areas thus confirming the conclusion made from the monolayer thickness measurements about the presence of the polymeric chain of DSPE-PEG5000 at the air/water interface in the true pancake conformation above ~ 37 nm²/molecule. Then, below 37 nm²/molecule, the slope of the $\ln \pi$ versus $\ln 1/A$ plot in Figure 4 changes. In regime II corresponding to the 34–25 nm²/molecule region of the π - A isotherm, we found a value of ~ 2.5 for the exponential factor γ that is in rather good correlation with the theoretically predicted value of $\gamma = 2.25$ for the quasi-3D layer.^{39,41} This is, therefore, a first indication that in the intermediate 34–25 nm²/molecule region preceding the plateau in the isotherm some of the $-(\text{CH}_2\text{CH}_2\text{O})-$ segments start submerging into the water subphase and thus a transition in the PEG5000 moiety conformation begins. The increase in monolayer thickness observed below 35 nm²/molecule (Figure 2) additionally supports the idea of gradual expulsion of PEG5000 chains into the subphase, leading to a conformation that results in a thicker layer. At this point, however, it is too early to draw any conclusions about

the nature of this transition. Although the conformation initially adopted by PEG5000 at the air/water interface has been identified as the pancake, we have yet to determine the resultant conformation that is developed at the end of the transition plateau.

4.2. Conformational Changes in PEG5000 Chains upon Compression. Conformational changes in a polymeric moiety at the air/water interface and molecular area ranges in which different conformations exist can be assessed in a first approximation by analyzing three major parameters that determine the conformation of grafted polymeric chains such as the polymer radius of gyration, R_g , the area per molecule in the monolayer, A , and the quality of the interface as a solvent. In general, at very large molecular areas, grafted polymeric chains will adopt either a pancakelike or a mushroomlike conformation depending on the interactions between their monomer segments and the quality of the interface as a solvent. However, when the area per molecule is reduced upon compression, closer contacts between neighboring molecules will induce stretching of polymeric chains, and at $A \approx \pi R_g^2/4$, a transition to brush conformation is expected.³ The polymer radius of gyration, therefore, can be considered to be a key parameter that determines the boundary between the nonoverlapping weakly interacting pancake/mushroom regime and the strongly interacting brush regime. For DSPE-PEG5000 that spreads into a true 2D layer at the air/water interface, the interface obviously acts as a good solvent,⁴³ and we may assess the PEG5000 radius of gyration using

$$R_g = an^{0.6} \quad (4)$$

where a is the monomer length and n is the degree of polymerization.⁴⁴ With $a = 0.35^8$ nm and $n = 110$, eq 4 yields $R_g \approx 5.8$ nm, thus setting the limit below which a transition to brush conformation should occur at $A \approx 27$ nm²/molecule. Given the fact that the plateau in the π - A isotherm in Figure 2 is observed well below 27 nm²/molecule, one might attribute this plateau to a pancake-to-brush conformational transition in the PEG5000 moiety. Indeed, according to the model proposed by Alexander, the compression of polymer-grafted monolayers may induce a first-order transition from the pancake-to-brush conformation that should appear as a plateau in π - A isotherms in the molecular area range given by

$$\chi_s^{0.5} < a^2 n \frac{1}{A} < (n \chi_s^6)^{0.14} \quad (5)$$

where χ_s is the adsorption energy per monomer.³⁸ For $-(\text{CH}_2\text{CH}_2\text{O})-$ monomers at the air/water interface, χ_s values were reported in the range of 0.6–1 units of kT .^{38,39} Hence, with a value of ~ 0.8 for χ_s , eq 5 predicts for DSPE-PEG5000 a first-order pancake-to-brush transition plateau in the ~ 15 – 8.5 nm²/molecule region. This calculated transition region superimposes fairly well the plateau observed in the ~ 18 – 5 nm²/molecule region of the DSPE-PEG5000 isotherm in Figure 2. However, the question is whether this plateau can be indeed ascribed to a first-order transition associated with the coexistence of two phases, namely, pancake regimes and brushes. As seen in Figure 2, the surface pressure continues to increase upon compression in the plateau, whereas in the case of a true first-order transition, π should remain independent of molecular area variation throughout the transition region. Yet, similar behavior was observed for a variety of lipid monolayers even when first-order phase transitions and phase coexistence did occur.³² To clarify this point, we analyzed the DSPE-PEG5000 isotherm

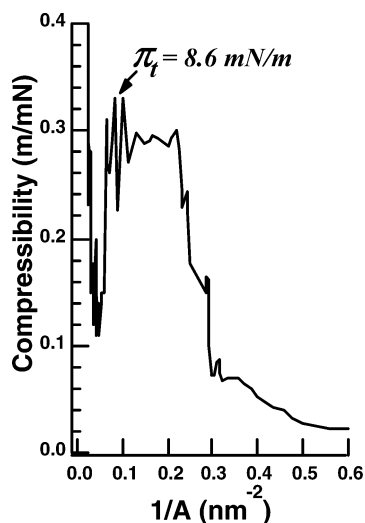


Figure 5. Plot of the monolayer compressibility, C , as a function of the reciprocal of molecular area. The compressibility was calculated from the slope of the π - A isotherm as given by $C = -1/A(\partial A/\partial \pi)_T$.⁵² The arrow indicates the region corresponding to the plateau onset in the π - A isotherm.

in terms of lateral area compressibility. The analysis yielded striking results. By contrast to a clear-cut peak expected for a first order transition, the plot of lateral area compressibility presented in Figure 5 exhibits only a break in the molecular area range corresponding to the isotherm plateau. This suggests that the plateau can be neither characterized as a first-order transition plateau⁴⁵ nor treated as a second-order transition. In fact, the lack of any peak at the plateau onset implies that this is not a true thermodynamic phase transition.

The hypothesis of a first-order pancake-to-brush conformational transition in the DSPE-PEG5000 monolayer is further confronted by the results of our BAM and AFM studies. As discussed above, both BAM and AFM images captured along the expanded region and plateau of the DSPE-PEG5000 isotherm invariably remained homogeneous. If the plateau corresponded to the coexistence of 2D pancake regimes and brushes, then this coexistence would be visualized, for instance, by BAM that derives contrast from differences in reflectivity between regions of different film density or thickness. Indeed, bright spots (denser and thicker areas) embedded in the darker background (more diluted areas) were observed in the plateau region for a polystyrene-PEO diblock copolymer containing PEO chains with $n = 700$ at the air/water interface.⁴¹ The fact that neither BAM nor AFM images of the DSPE-PEG5000 monolayer show any sign of phase coexistence makes the interpretation of the plateau in terms of first-order pancake-to-brush transition rather doubtful. A similar conclusion was made in previous studies performed with medium-sized PEG grafted chains ($n \leq 400$) at the air/water interface.^{38,41}

Additional analysis of experimental data obtained in the present study raises more doubts about the possibility of a transition from pancake to brush conformation. Indeed, the assumption of the pancake-to-brush transition, especially if one refers to a first-order transition, implies that PEG chains remain extended at the interface, with every monomer segment in the surface layer, up to the onset of conformational transition. Although compression may cause a gradual entanglement, the polymeric chains are supposed to stay at the interface until a dense 2D entangled layer is formed. Then, brushes begin developing spontaneously from entangled pancakes, pushing the distal end of the polymeric chain into the subphase.³⁸ As this transition sets in, the surface pressure should level off, marking

the onset of the plateau in π - A isotherms. Clearly, the results presented in Figures 2 and 4 do not agree with this scenario. As discussed above, changes in the conformation of the PEG moiety begin at approximately 35 nm²/molecule, thus long before the onset of the isotherm plateau at ~ 18 nm²/molecule. Yet, neither surface pressure nor ellipsometry data provide any evidence for the formation of a 2D entangled layer in the intermediate 35–18 nm²/molecule region preceding the plateau. Instead, a gradual expulsion of PEG chains into the subphase resulting in the formation of a quasi-3D layer is suggested by the surface pressure exponent $\gamma = 2.5$ (see regime II in Figure 4 and the related discussion above) and the thickening of the DSPE-PEG5000 monolayer below 35 nm²/molecule. As seen in Figure 2, at the onset of the isotherm plateau, a value of ~ 3.3 nm was obtained for the monolayer thickness, which is approximately 3 times larger than the thickness of a true 2D DSPE-PEG5000 monolayer (~ 0.9 nm). On the basis of this finding, one might then discuss the plateau in light of a transition between a quasi-3D overlapping regime and a quasi-brush.⁴⁰ This model, however, predicts that in the quasi-brush regime polymeric chains are stretched to about $2R_g$.⁴⁰ Given the R_g value of 5.8 nm as calculated using eq 4, a value of ~ 11.6 nm would be expected for the height of the PEG5000 brush. By contrast, filled circles in Figure 2 show that at the end of the isotherm plateau the thickness of the DSPE-PEG5000 monolayer reaches a value of 6.8 nm, which is barely comparable to the PEG5000 radius of gyration. This small value of monolayer thickness also disagrees with the Alexander theory that provides even larger estimates for the polymer brush height.

Although our experimental data do not provide evidence strongly supporting the idea of a pancake-to-brush transition in the DSPE-PEG5000 monolayer at the air/water interface, the close correlation between the monolayer thickness and the R_g value suggests the possibility of a PEG5000 mushroom formation in the plateau region of the π - A isotherm. In fact, previous studies interpreted the plateau typically observed in π - A isotherms of PEG-phospholipid conjugates at $\pi \approx 8.6$ mN/m as a transition between the pancake and mushroom conformations in PEG5000.^{9,12,17} Yet, despite an increasing number of reports referring to the pancake-to-mushroom transition, no unequivocal experimental evidence has been presented supporting this concept. This transition has not been well defined theoretically. Therefore, at this point, our assumption of a PEG5000 mushroom formation in the plateau region of the π - A isotherm is based solely on a general idea of scaling approaches that the thickness of a polymer layer is scaled by R_g if the layer is in the mushroom regime.^{9,46} A better view of polymeric chain extension into the subphase and conformational changes in PEG5000 can be obtained from the comparative analysis of π - A isotherm and ellipsometry data in terms of radii of gyration of the PEG5000 moiety in the monolayer plane, $R_{g,xy}$, and along the interface normal, $R_{g,z}$. Figure 6 shows a schematic diagram of changes in the average shape of the PEG5000 moiety upon compression. The diagram displays an interesting sequence of shape changes where the extension of the PEG5000 chain into the subphase increases continuously throughout the 35–5 nm²/molecule region of the DSPE-PEG5000 isotherm. As seen in the Figure, the average conformation formed at the onset of the isotherm plateau (shape b) can indeed be viewed as somewhat similar to the hemispherical mushroom described by de Gennes. However, the size of the PEG5000 mushroom determined by $R_{g,xy} \approx 4.9$ nm and $R_{g,z} \approx 3.3$ nm (as estimated from π - A isotherm and ellipsometric measurements of monolayer thickness, respectively) is surprisingly small compared to

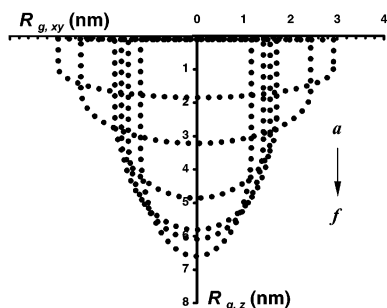


Figure 6. Average shapes of the PEG5000 moiety at different surface pressures on approaching the isotherm plateau and in the plateau region: (a) $A = 28 \text{ nm}^2/\text{molecule}$, $\pi = 2.7 \text{ mN/m}$; (b) $A = 18.5 \text{ nm}^2/\text{molecule}$, $\pi = 6.9 \text{ mN/m}$; (c) $A = 9 \text{ nm}^2/\text{molecule}$, $\pi = 9.3 \text{ mN/m}$; (d) $A = 7.7 \text{ nm}^2/\text{molecule}$, $\pi = 9.7 \text{ mN/m}$; (e) $A = 6.5 \text{ nm}^2/\text{molecule}$, $\pi = 10.1 \text{ mN/m}$; (f) $A = 5 \text{ nm}^2/\text{molecule}$, $\pi = 12 \text{ mN/m}$. The radius of gyration of the PEG5000 moiety in the monolayer plane, $R_{g,xy}$, was roughly estimated from the π - A isotherm as $R_{g,xy}^2 = A/3.1416$, although for the radius of gyration along the interface normal, $R_{g,z}$, it was assumed that $R_{g,z} \approx d$, where d is the monolayer thickness measured at given A and π . The shapes are drawn schematically on the basis of the results of neutron reflectivity studies⁷ suggesting the density profile of the PEG5000 chains to be of a parabolic type.

the 3D radius of gyration, $R_g \approx 5.8 \text{ nm}$, predicted by eq 4 for PEG5000 in a good solvent. Further compression throughout the plateau region causes noticeable lateral deformation in the average shape of the PEG5000 mushroom (shapes c throughout f in Figure 6). Eventually, an elongated conformation is developed at the end of the isotherm plateau (Figure 6f). Comparing the radius of gyration in the monolayer plane, $3.2 < R_{g,xy} < 2.5 \text{ nm}$, to that along the interface normal, $6.1 < R_{g,z} < 6.8$, for the PEG5000 moiety at the end of the DSPE-PEG5000 isotherm plateau ($5 \text{ nm}^2/\text{molecule}$), we found the extension of the polymeric chain along the interface normal to be some 2- to 3-fold greater than that in the monolayer plane. Following the classification suggested in the literature, such a configuration can be described as an extended mushroom.^{8,46} However, assuming that the effective 3D radius of gyration of the PEG5000 moiety at the air/water interface R_g is virtually equal to $R_{g,z}$ at the onset of the isotherm plateau ($\sim 3.3 \text{ nm}$ (shape b)) as opposed to the value of 5.8 nm predicted by eq 4, one can also describe the conformation of the PEG5000 moiety at the end on the plateau as a quasi-brush³⁹⁻⁴¹ because its extension into the subphase is about $2R_g$, where $R_g \approx 3.3 \text{ nm}$. The sequence of shape changes revealed by the comparative analysis of π - A isotherm and ellipsometric data therefore enables us to conclude that, as the transition begins, PEG5000 chains undergo continuous changes in their average conformation from 2D pancakes to extended mushrooms or quasi-brushes. It is noteworthy that the conformation developed at the end of the transition plateau differs from both mushroom and brush. Although relatively elongated, the PEG5000 moiety is much less extended into the subphase (~ 6.1 – 6.8 nm) than would be expected for a true brush (~ 10 – 12.7 nm for PEG5000^{3,6,7,11,46}). One might argue that the extension of the PEG5000 chain into the subphase was underestimated in our study, given that it was assessed on the basis of ellipsometric measurements of monolayer thickness. In particular, the hydration of headgroups and PEG5000 chains could render the refractive index of a part of the monolayer hydrophilic region close to that of the water subphase, thus making it undetectable by ellipsometry. However, we shall point out that the value of $6.8 \pm 0.5 \text{ nm}$ for the thickness of the DSPE-PEG5000 monolayer at $5 \text{ nm}^2/\text{molecule}$ obtained by ellipsometry is in fairly good correlation with a

value of 7.4 nm at $4.6 \text{ nm}^2/\text{molecule}$ measured by X-ray reflectivity in previous studies.¹¹

4.3. Quality of the Air/Water Interface as a Solvent and Its Effect on the PEG5000 Chain Conformation. An interesting finding is that the dimensions of the PEG5000 moiety at the air/water interface differ significantly from the theoretical predictions for both the PEG5000 mushroom radius and PEG5000 brush height made under the assumption of the air/water interface as a good-quality solvent for PEG chains. In particular, although the average conformation developed at the onset of the isotherm plateau resembles a mushroom, its 3D radius of gyration roughly estimated from the ellipsometric data as $R_g \approx 3.3 \text{ nm}$ is a factor of 1.8 smaller than the R_g value calculated from eq 4 ($R_g \approx 5.8 \text{ nm}$). The conformation developed at the end of the isotherm plateau, if viewed as a brush, is also less extended (twice as much) into the subphase than is expected for the PEG5000 brush in a good solvent. A plausible explanation for the discrepancy between the theoretical values and the measured monolayer thickness may be a surface-crowding induced change in the quality of the air/water interface as a solvent for PEG chains, which has not yet been accounted for. As pointed out by Lai et al.,⁴⁷ most of the theoretical concepts suggested in the literature have been mainly focused on how the conformation of grafted polymeric chains is affected by their size and grafting density, assuming the grafted layers to be in a good solvent, although solvent quality is obviously another important part of the problem. Indeed, when the area available per molecule in the monolayer is large enough for every PEG5000 chain to extend at the air/water interface, the interface acts as a good solvent, and polymeric chains adopt the 2D pancake conformation. Upon compression, however, the interface becomes more and more crowded with PEG chains, and its quality as a solvent very likely decreases.^{42,47} For instance, it has been proven for PEO aqueous solutions that although water is a good solvent for PEOs its quality as a solvent decreases with increasing concentration of the polymer.^{42,48} The effect that changes in solvent quality may have on the conformation of polymeric chains is that as the solvent quality changes from good to worse polymeric chains tend to form more compact conformations.^{47,48}

In general, interactions between the polymeric chain and the solvent are characterized by the Flory exponent, ν , which relates the polymer's 3D radius of gyration, R_g , to the size of the monomer segment, a , and the degree of polymerization, n , as

$$R_g = an^\nu \quad (6)$$

According to the predictions of scaling theories, the Flory exponent decreases with decreasing solvent quality from $\nu = 0.6$ for a good solvent (in this case, eq 6 gives eq 4 used earlier to assess the R_g value for PEG5000) to $\nu = 0.5$ and 0.3 for theta and bad solvents, respectively.^{44,47} By analogy, for polymeric chains grafted at the interface, changes in the solvent quality from good to bad will result in a shrinkage of polymer mushrooms and, consequently, in a thinner layer because the polymer layer thickness in the mushroom regime is scaled by R_g . Polymer brushes will also be less stretched in theta and bad solvents than in good solvents. The height of a polymer brush can be determined for different solvent conditions using

$$H_{\text{brush}} = an \left(\frac{a^2}{A} \right)^w \quad (7)$$

where the exponential factor w varies depending on the solvent quality.^{44,47} For a good solvent, $w = 0.3$ whereas for a theta or

a bad solvent, $w = 0.5$ or 1 , respectively.⁴⁴ Hence, assuming that the quality of the air/water interface as a solvent changes upon monolayer compression from good to theta, we obtain a value of ~ 3.7 nm for the PEG5000 radius of gyration (theta solvent conditions) instead of 5.8 nm calculated from eq 4 (good solvent conditions). The comparison of the experimental data in Figures 2 and 6 with the calculated values for R_g shows that the calculated R_g value of 3.7 nm is in good correlation with the value of 3.3 nm obtained for monolayer thickness at the onset of the isotherm plateau. Moreover, the height of PEG5000 brushes, H_{brush} , estimated from eq 7 assuming theta solvent conditions also agrees fairly well with the thickness of the DSPE-PEG5000 monolayer measured at the end of the isotherm plateau. Indeed, with $w = 0.5$, eq 7 predicts $H_{\text{brush}} \approx 6.1$ nm for the PEG5000 brush at the end of the plateau. Comparing this value with the measured monolayer thickness found in the range of 6.2–6.8 nm (at the end of the isotherm plateau, Figure 2), one can clearly see that the prediction of the theta solvent approximation is in much better agreement with the experimental data than values of ~ 10 –12.7 nm calculated using good solvent approximations.^{6,7,11} The assumption of decreasing quality of the air/water interface as a solvent upon compression therefore makes sense.

Decreasing quality of the air/water interface as a solvent implies that as the interface gets more crowded with the PEG chains the interactions between $-(\text{CH}_2\text{CH}_2\text{O})-$ segments and water molecules change. Presumably, to relax the lateral stress and repulsion between neighboring PEG chains due to excluded volume interactions upon compression, the PEG5000 chain not only displaces its monomer segments into the subphase adopting quasi-3D conformations (i.e., mushroom or brush) but also gives up some of the water molecules of its hydration shell. The conformational change in PEG5000 chains grafted onto the phospholipid monolayer that occurs upon compression can therefore be described as a transition from a pancake to a poorly hydrated brush conformation that eventually develops at the end of the isotherm plateau. At this point, we cannot say unambiguously which route the transition takes: whether it goes from a pancake to a semihydrated mushroom and then to a poorly hydrated brush or whether it is a broad pancake-to-poorly hydrated-brush transition. A more important finding, however, is that the transition is accompanied by the dehydration of PEG5000 chains, which is almost equivalent to the change in the solvent quality from good to theta. A similar conclusion was made previously for PEG2000 chains grafted onto phospholipid monolayers.¹⁷ To estimate quantitatively the changes associated with the dehydration of the PEG5000 chain upon compression, we used an approach similar to the mass conservation law. We used the average chain volume (ACV = area per molecule \times monolayer thickness) as the major parameter to determine the changes in the average volume occupied by the PEG5000 chain roughly upon compression. At the beginning of the isotherm, $\text{ACV} = 45 \text{ nm}^3$, whereas at the end of the isotherm plateau (prior to the monolayer collapse), $\text{ACV} = 34 \text{ nm}^3$. We believe that this decrease in the ACV value is indicative of the expulsion of some of the water molecules out of the PEG5000 hydration shell upon compression.

4.4. Cooperative Changes in the Conformation and Hydration of PEG5000 Chains upon Compression. The idea of changes in the hydration of PEG5000 with increasing grafting density is additionally supported by our surface potential data. As discussed earlier, the dipole moment sum, $\mu_{\text{PEG}}/\epsilon_{\text{PEG}} + \mu_{\text{H}_2\text{O}}/\epsilon_{\text{H}_2\text{O}}$, calculated from the surface potential data can be used to determine changes in the conformation and hydration of

PEG5000 chains upon compression. The dependence of $\mu_{\text{PEG}}/\epsilon_{\text{PEG}} + \mu_{\text{H}_2\text{O}}/\epsilon_{\text{H}_2\text{O}}$ as a function of molecular area is demonstrated by curve f in Figure 3. It is noteworthy that both at large molecular areas and at the end of the π -A isotherm plateau the values of $\mu_{\text{PEG}}/\epsilon_{\text{PEG}} + \mu_{\text{H}_2\text{O}}/\epsilon_{\text{H}_2\text{O}}$ were very high. At the lift off of the ΔV -A isotherm, the value of $\mu_{\text{PEG}}/\epsilon_{\text{PEG}} + \mu_{\text{H}_2\text{O}}/\epsilon_{\text{H}_2\text{O}}$ was as high as 31 D, and it remained almost unchanged in the 50–35 $\text{nm}^2/\text{molecule}$ region. Below 35 $\text{nm}^2/\text{molecule}$, on approaching the π -A isotherm plateau and in the plateau region, the dipole moment sum decreased continuously down to a value of ~ 5 D, which was eventually attained at 5 $\text{nm}^2/\text{molecule}$.

Regardless of the partitioning of the constituent parts of eq 2, the dipole moment sum might be constant only if the conformation of the polymeric moiety as well as the orientation of water molecules was not altered to any significant extent upon compression.³⁰ According to the analysis of the π -A isotherm and ellipsometric data discussed above, the conformation of PEG5000 chains remained unchanged in the 50–35 $\text{nm}^2/\text{molecule}$ region corresponding to the 2D pancake regime. Given that $\mu_{\text{PEG}}/\epsilon_{\text{PEG}} + \mu_{\text{H}_2\text{O}}/\epsilon_{\text{H}_2\text{O}}$ also remained constant in the same molecular area range, we believe the value of ~ 31 D to be characteristic of the PEG5000 chain in the pancake conformation. Therefore, such a large positive dipole moment must be due to an additive contribution of individual $-(\text{CH}_2\text{CH}_2\text{O})-$ dipoles of the PEG chain and the presence of ordered water molecules in its hydration shell. Although the PEG5000 chain itself consists of 110 monomers, each of which has a dipole moment of ~ 1.2 D directed along the chain,⁴⁹ it cannot produce a substantial group dipole moment $\mu_{\text{PEG}}/\epsilon_{\text{PEG}} + \mu_{\text{H}_2\text{O}}/\epsilon_{\text{H}_2\text{O}}$. Indeed, in the pancake conformation, when the chain is extended at the interface, dipole moments of $-(\text{CH}_2\text{CH}_2\text{O})-$ segments are oriented essentially parallel to the interface. This orientation will result in a small normal component of the $-(\text{CH}_2\text{CH}_2\text{O})-$ dipole moment,^{26,31} thus diminishing substantially the contribution of $-(\text{CH}_2\text{CH}_2\text{O})-$ dipoles to $\mu_{\text{PEG}}/\epsilon_{\text{PEG}} + \mu_{\text{H}_2\text{O}}/\epsilon_{\text{H}_2\text{O}}$. The unusually high value of ~ 31 D for $\mu_{\text{PEG}}/\epsilon_{\text{PEG}} + \mu_{\text{H}_2\text{O}}/\epsilon_{\text{H}_2\text{O}}$ therefore implies a significant positive contribution from ordered water dipoles.^{30,37,43,50} Recently, Fourier transform infrared study and NMR relaxation time measurements^{35,36} revealed not only that water molecules bind to the oxygen atom of $-(\text{CH}_2\text{CH}_2\text{O})-$ monomers forming the PEG hydration shell but also that free water molecules associate with the hydration shell. Consequently, a large-scale reorientation of water molecules is expected to occur in the vicinity of the PEG-grafted monolayer. Given that every water molecule has a dipole moment of 1.8 D,⁵⁰ altogether normal components of dipole moments of water molecules of the polymer hydration shell can contribute with tens of debyes to the dipole moment sum, thus producing high values of $\mu_{\text{PEG}}/\epsilon_{\text{PEG}} + \mu_{\text{H}_2\text{O}}/\epsilon_{\text{H}_2\text{O}}$.

By contrast, the decrease in $\mu_{\text{PEG}}/\epsilon_{\text{PEG}} + \mu_{\text{H}_2\text{O}}/\epsilon_{\text{H}_2\text{O}}$ below 35 $\text{nm}^2/\text{molecule}$ is obviously related to the gradual expulsion of PEG5000 chains into the subphase followed by the transition to quasi-3D conformation(s) and changes in hydration. In fact, the conformational transition in the polymeric chain leads to a smaller degree of orientation of $-(\text{CH}_2\text{CH}_2\text{O})-$ dipoles perpendicular to the interface.¹⁶ Because PEG becomes a coil in the aqueous subphase, orientational disorder may be a reason for $-(\text{CH}_2\text{CH}_2\text{O})-$ dipoles to cancel each other partially. At the same time, the hydration number of PEG decreases because it depends on the chain conformation.^{35,36} In the pancake conformation, $-(\text{CH}_2\text{CH}_2\text{O})-$ monomers are more accessible to water and, presumably, more hydrated than in quasi-3D conformations. Moreover, because water molecules participate in the packing of PEG chains,^{35,36} the conformational transition

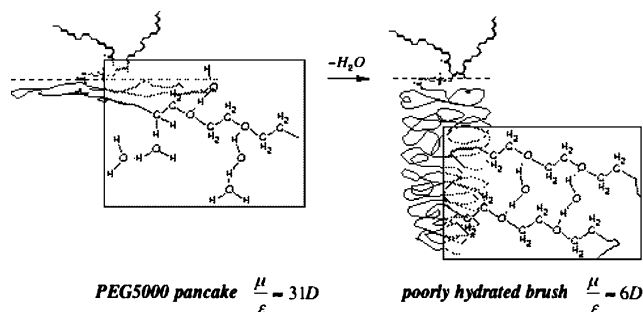


Figure 7. Changes in interactions of PEG5000 with water molecules and the dehydration of PEG5000 chains grafted onto the phospholipid monolayer upon compression. At low grafting densities, when the chain is in the pancake conformation, both water binding to $-(CH_2CH_2O)-$ monomers and unbound water molecules associating with the binding water are present in the polymer hydration shell. With increasing grafting density, however, a large body of water is likely to be squeezed out of the PEG hydration shell, and the rest will participate in the packing of PEG5000 chains in quasi-3D conformations bridging $-(CH_2CH_2O)-$ segments. The drawing is made on the basis of results of previous studies.^{35,36}

will probably cause the complete loss of unbound water in the PEG hydration shell and the appearance of bridging water molecules cross linking PEG chain segments instead of binding water hydrating individual $-(CH_2CH_2O)-$ monomers. A schematic view of the changes in the hydration of PEG5000 chains upon the transition from pancake to poorly hydrated brush conformation is depicted in Figure 7. Eventually, these kinds of changes in the hydration should significantly reduce the contribution of water dipoles to $\mu_{PEG}/\epsilon_{PEG} + \mu_{H_2O}/\epsilon_{H_2O}$, which is consistent with the decrease in the dipole moment sum that begins on approaching the π -A isotherm plateau and becomes even more pronounced upon further compression throughout the plateau (Figure 3, curve f).

An unusual trend of decreasing the absolute value of the ψ_0 potential with reducing molecular area (curve e in Figure 3) also supports the concept of progressive changes in the PEG hydration upon compression. Because the phosphoethanolamine headgroup (PE) of DSPE-PEG5000 is negatively charged, the ψ_0 potential is expected to become more and more negative as the surface density of PE groups is increased (with decreasing area per molecule upon compression).^{6,51} The observed opposite trend appears to be counterintuitive. However, assuming the transition from the highly hydrated pancake conformation to the poorly hydrated brush discussed above, it is plausible that the decrease in the ψ_0 potential is related to a change in the local dielectric constant of the headgroup region. Pure PEO has a dielectric constant of $\epsilon = 11$, which is much lower than that of water ($\epsilon = 80$).⁶ Hence, because the expulsion of polymer chains from the interface followed by the formation of quasi-3D conformations may alter the hydration of PEG, the dielectric constant of the medium surrounding the charged PE groups will probably decrease. According to Kuhl at al.,⁶ the overall effect of this local decrease in ϵ would be a lower degree of PE group dissociation and, consequently, a lower surface charge density at the interface, which would lead to the observation of the decrease in the ψ_0 potential upon compression.

Conclusions

In the present study, we investigated conformations of a PEG chain with molecular mass 5000 grafted onto a phospholipid in monolayers at the air/water interface. The comparative analysis of π -A and ΔV -A isotherms and ellipsometric, BAM, and AFM data provided new insights into the nature of the

conformational transition occurring in the monolayer of a PEG-phospholipid, DSPE-PEG5000, when the grafting density of PEG5000 chains increased upon compression. Whereas at low grafting densities PEG5000 chains behaved as grafted polymeric chains in a good solvent forming true 2D pancakes at the air/water interface, the conformation developed at high grafting densities was found to differ significantly from both mushroom and brush. Although relatively elongated, this conformation is less extended into the subphase than expected for the PEG5000 brush in a good solvent. At high grafting densities, the extension of PEG5000 chains into the subphase is in far better agreement with the theoretical predictions for the height of PEG5000 brush in a theta solvent. This finding together with the progressively decreasing dipole moment of PEG5000 enabled us to conclude that as grafting density increased the PEG chain not only displaced its monomer segments into the subphase adopting quasi-3D conformations (i.e., mushroom or brush) but also gave up some of the water molecules of its hydration shell. The conformational change in PEG5000 chains grafted onto the phospholipid monolayer can therefore be described as a transition from a highly hydrated pancake to a poorly hydrated brush conformation. This transition was also reflected in the electrostatic properties of DSPE-PEG5000. Indeed, an unusual trend of decreasing absolute value of the electric double-layer ψ_0 potential observed at high PEG grafting densities is believed to be due to the dehydration of PEG chains upon transition to quasi-3D conformations, which caused a decrease in the dielectric constant of the monolayer headgroup region and, consequently, a lower degree of DSPE-PEG5000 headgroup dissociation.

The dehydration of PEG5000 chains upon increasing surface density may have implications for understanding interactions of PEG-grafted membrane-mimetic surfaces with proteins. In particular, our results suggest that the explanation for the repeatedly reported adsorption of certain proteins on PEG5000-grafted bilayers and liposomes may be associated with the appearance of protein-attractive hydrophobic sites on the surface as a result of the poor hydration of PEG5000 chains in the mushroom and brush conformations. However, to verify this possibility, additional investigations need to be conducted.

Acknowledgment. We thank the Natural Sciences and Engineering Research Council of Canada for the financial support of this study. C.S. is a chercheur boursier national of the Fonds de recherche en santé du Québec. An invitation fellowship of the Centre de Recherche en Sciences et Ingénierie des Macromolécules (Quebec, Canada) to V.T. is gratefully acknowledged. We are grateful to P. Basque for the scanning and processing of AFM images. We also thank Dr. D. Ducharme for his collaboration in the ellipsometric experiments and S. Senkow for helping out with the preparation of deposited films.

References and Notes

- (1) Harris, J. M., Ed. *Poly(ethylene glycol) Chemistry: Biotechnical and Biomedical Applications*; Plenum Press: New York, 1992.
- (2) Collier, J. H.; Messersmith, P. B. *Annu. Rev. Mater. Res.* **2001**, *31*, 237.
- (3) Vermette, P.; Meagner, L. *Colloids Surf., B* **2003**, *28*, 153.
- (4) Efremova, N. V.; Sheth, S. R.; Leckband, D. E. *Langmuir* **2001**, *17*, 7628.
- (5) Zhao, H.; Dubielecka, P. M.; Söderlund, T.; Kinnunen, P. K. J. *Biophys. J.* **2002**, *83*, 954.
- (6) Kuhl, T. L.; Leckband, D. E.; Lasic, D. D.; Israelachvili, J. N. *Biophys. J.* **1994**, *66*, 1479.
- (7) Bianco-Peled, H.; Dori, Y.; Schneider, J.; Sung, L.-P.; Satija, S.; Tirrell, M. *Langmuir* **2001**, *17*, 6931.

- (8) Rex, S.; Zuckermann, M. J.; Lafleur, M.; Silvius, J. R. *Biophys. J.* **1998**, *75*, 2900.
- (9) Baekmark, T. R.; Elender, G.; Lasic, D. D.; Sackmann, E. *Langmuir* **1995**, *11*, 3975.
- (10) Harder, P.; Grunze, M.; Dahint, R.; Whitesides, G. M.; Laibinis, P. E. *J. Phys. Chem. B* **1998**, *102*, 426.
- (11) Ahrens, H.; Baekmark, T. R.; Merkel, R.; Schmitt, J.; Graf, K.; Raiteri, R.; Helm, C. *ChemPhysChem* **2000**, *2*, 101.
- (12) Baekmark, T. R.; Wiesenenthal, T.; Kuhn, P.; Albersdörfer, A.; Nuyken, O.; Merkel, R. *Langmuir* **1999**, *15*, 3616.
- (13) Wiesenenthal, T.; Baekmark, T. R.; Merkel, R. *Langmuir* **1999**, *15*, 6837.
- (14) Bürner, H.; Winterhalter, M.; Benz, R. *J. Colloid Interface Sci.* **1994**, *168*, 183.
- (15) Tsukanova, V.; Salesse, C. *Macromolecules* **2003**, *36*, 7227.
- (16) Winterhalter, M.; Bürner, H.; Marzinka, S.; Benz, R.; Kasianowicz, J. J. *Biophys. J.* **1995**, *69*, 1372.
- (17) Xu, Z.; Holland, N. B.; Marchant, R. E. *Langmuir* **2001**, *17*, 377.
- (18) Rosilio, V.; Albrecht, G.; Okumura, Y.; Sunamoto, J.; Baszkin, A. *Langmuir* **1996**, *12*, 2544.
- (19) Gallant, J.; Lavoie, H.; Tessier, A.; Munger, G.; Leblanc, R. M.; Salesse, C. *Langmuir* **1998**, *14*, 3954.
- (20) Ducharme, D.; Tessier, A.; Russev, S. *Langmuir* **2001**, *17*, 7529.
- (21) Kawaguchi, M.; Tohyama, M.; Mutoh, Y.; Takahashi, A. *Langmuir* **1988**, *4*, 407.
- (22) Kawaguchi, M.; Tohyama, M.; Takahashi, A. *Langmuir* **1988**, *4*, 411.
- (23) Muñoz, M. G.; Monroy, F.; Ortega, F.; Rubio, R. G.; Langevin, D. *Langmuir* **2000**, *16*, 1083.
- (24) Nagata, K.; Kawaguchi, M. *Macromolecules* **1990**, *23*, 3957.
- (25) Gaines, G. L., Jr. *Langmuir* **1991**, *7*, 834.
- (26) Vogel, V.; Möbius, D. *J. Colloid Interface Sci.* **1988**, *126*, 408.
- (27) Vogel, V.; Möbius, D. *Thin Solid Films* **1985**, *132*, 205.
- (28) Dynarowicz-Latka, P.; Dhanabalan, A.; Cavalli, A.; Oliveira, O. N., Jr. *J. Phys. Chem. B* **2000**, *104*, 1701.
- (29) Oliviera, O. N., Jr.; Taylor, D. M.; Stirling, C. J. M.; Tripathi, S.; Guo, B. Z. *Langmuir* **1992**, *8*, 1619.
- (30) Brockman, H. *Chem. Phys. Lipids* **1994**, *73*, 57.
- (31) Tocanne, J.-F.; Teissie, J. *Biochim Biophys. Acta* **1990**, *1031*, 111.
- (32) Tsukanova, V.; Grainger, D. W.; Salesse, C. *Langmuir* **2002**, *18*, 5539.
- (33) Demchak, R. J.; Fort, T., Jr. *J. Colloid Interface Sci.* **1974**, *46*, 191.
- (34) Helm, C. A.; Möhwal, H.; Kjaer, K.; Als-Nielsen, J. *Europhys. Lett.* **1987**, *4*, 697.
- (35) Kitano, H.; Ichikawa, K.; Ide, M.; Fukuda, M.; Mizuno, W. *Langmuir* **2001**, *17*, 1889.
- (36) Lüsse, S.; Arnold, K. *Macromolecules* **1996**, *29*, 4251.
- (37) Alper, H. E.; Bassolino-Klimas, D.; Stouch, T. R. *J. Chem. Phys.* **1993**, *99*, 5547.
- (38) Bijsterbosch, H. D.; de Haan, V. O.; de Graaf, A. W.; Mellema, M.; Leermakers, F. A. M.; Cohen Stuart, M. A.; van Well, A. A. *Langmuir* **1995**, *11*, 4467.
- (39) Fauré, M. C.; Bassereau, P.; Carignano, M. A.; Szleifer, I.; Gallot, Y.; Andelnam, D. *Eur. Phys. J. B* **1998**, *3*, 365.
- (40) Gonçalves da Silva, A. M.; Filipe, E. J. M.; d'Oliveira, J. M. R.; Martinho, J. M. G. *Langmuir* **1996**, *12*, 6547.
- (41) Fauré, M. C.; Bassereau, P.; Lee, L. T.; Menelle, A.; Lheveder, C. *Macromolecules* **1999**, *32*, 8538.
- (42) Barentin, C.; Muller, P.; Joanny, J. F. *Macromolecules* **1998**, *31*, 2198.
- (43) Esker, A. R.; Zhang, L.-H.; Sauer, B. B.; Lee, W.; Yu, H. *Colloids Surf., A* **2000**, *171*, 131.
- (44) Chern, S.-S.; Zhulina, E. B.; Pickett, G. T.; Balazs, A. C. *J. Chem. Phys.* **1998**, *108*, 5981.
- (45) Haas, F. M.; Hilfer, R.; Binder, K. *J. Phys. Chem.* **1996**, *100*, 15290.
- (46) Carignano, M. A.; Szleifer, I. *Macromolecules* **1995**, *28*, 3197.
- (47) Lai, P.-Y.; Binder, K. *J. Chem. Phys.* **1992**, *97*, 586.
- (48) Smith, G. D.; Bedrov, D.; Borodin, O. *J. Am. Chem. Soc.* **2000**, *122*, 9548.
- (49) Kolafa, J.; Ratner, M. *Mol. Simul.* **1998**, *21*, 1.
- (50) Gawrisch, K.; Ruston, D.; Zimmerberg, J.; Parsegian, V. A.; Rand, R. P.; Fuller, N. *Biophys. J.* **1992**, *61*, 1213.
- (51) Aguilera, V. M.; Mafé, S.; Manzanares, J. A. *Chem. Phys. Lipids* **2000**, *105*, 225.
- (52) Gaines, G. L., Jr. *Insoluble Monolayers at Liquid-Gas Interfaces*; Wiley: New York, 1966.